Atomic forces at finite magnetic temperatures: Phonons in paramagnetic iron

F. Körmann,[1,*] A. Dick,[1] B. Grabowski,[2] T. Hickel,[1] and J. Neugebauer[1]

[1]*Max-Planck-Institut für Eisenforschung GmbH, D-40237 Düsseldorf, Germany*
[2]*Lawrence Livermore National Laboratory (L-280), P.O. Box 808, Livermore, California 94550, USA*

A density-functional theory (DFT) based scheme to calculate effective forces for magnetic materials at finite temperatures is proposed. The approach is based on a coarse graining procedure in the magnetic configuration space. As application we calculate phonon spectra of paramagnetic bcc and fcc iron and show good agreement with experimental data.

Accurate and efficient computational schemes for the theoretical prediction of parameter-free atomic forces and force constants are an essential prerequisite for many applications within first-principles materials design, such as lattice vibrations (phonon spectra, vibronic entropies, phase transitions),[1–13] diffusion processes (vacancies, impurities, etc.),[14] strain fields (e.g., in grain boundaries), or even fundamental methods such as molecular dynamics (MD) simulations.[15–17]

Although nowadays powerful tools exist to compute and extract forces and force constants (direct force constant approach/linear-response theory,[18] *ab initio* MD[19]), current approaches are often not suited for describing magnetic materials at finite temperatures, i.e., under conditions away from the magnetic ground state. A prominent example is the paramagnetic regime. Due to the lack of alternatives, current theoretical approaches for, e.g., vibronic contributions of magnetic materials such as bcc iron, rely on calculations performed in the magnetic ground state (e.g., the ferromagnetically saturated state),[13,20] or take the missing data from experiment.[7] Approaches going beyond these simple approximations employ fixed-spin calculations[6,21] or GGA + U,[5] but still employ magnetically fully ordered configurations. Although it is known that magnetism can have a substantial impact on vibrational properties,[22,23] the basic fundamentals are still poorly understood.[5,8,23]

A state-of-the-art first-principles approach to study magnetically disordered systems is the coherent potential approximation (CPA) (a recent review is given, e.g., in Ref. 24). In combination with the so-called disordered local moment (DLM) model, the magnetically disordered system is modeled as an effective medium of spin-up and spin-down species.[25] An inherent limitation of the CPA treatment is that a direct evaluation of forces and force constants is not possible due the single-site nature of this approach.[24] This seriously limits the approach when applied to systems for which relaxation effects become important.

Recently, Shang *et al.*[26] proposed for magnetic systems at elevated temperatures an approach to determine macroscopic thermodynamic properties such as free energies and specific-heat capacities. In their approach a Boltzmann statistical averaging of free energies of individual magnetic microstates, such as ferromagnetic or antiferromagnetic states, is performed. Individual force and phonon calculations are performed for each microstate independently. This approach implicitly assumes that in each microstate "fast" atoms move in a "fixed"

magnetic configuration. This assumption does not hold at high temperatures, where the magnitude of typical magnetic excitations is higher in energy than vibronic excitations, implying a faster time scale for the magnetic degree of freedom.[11,12,27] A very recent theoretical approach by Leonov *et al.* which takes magnetic correlations in force constant calculations within the framework of dynamical mean-field theory into account, provides promising preliminary results for fcc iron.[28] This method is, however, still under development.

In this paper we propose an approach that overcomes the limitations of current theoretical treatments and that can be easily implemented in existing DFT codes. We start from the magnetic Born-Oppenheimer (BO) energy surface $E^{\mathrm{BO}}(\{\vec{R}_I\},\vec{\sigma})$ within constrained spin density-functional theory, which denotes the unique total energy for a given set of atomic coordinates $\{\vec{R}_I\}$ and local magnetic moments $\vec{\sigma} = \{\sigma_I\}$. As a first step we discretize and coarse grain the (principally infinite) configurational spin space and define a spin space averaged (SSA) free-energy energy as

$$\mathcal{F}^{\mathrm{SSA}}_{\{\vec{R}_I\}} = -k_{\mathrm{B}}T \, \ln Z, \tag{1}$$

where $Z = \sum_m \exp[-E^{\mathrm{BO}}(\{\vec{R}_I\},\vec{\sigma}_m)/k_{\mathrm{B}}T]$ denotes the magnetic partition sum and m indexes the individual magnetic configurations. Note that the SSA free energy is not equivalent to the full free energy (which would have to include, e.g., vibronic excitations).

A major advantage of this formulation is that atomic forces on an atom J are directly accessible as gradients on the SSA free energy BO surface:

$$\vec{F}^{\mathrm{SSA}}_{J,\{\vec{R}_I\}} = -\frac{\partial \mathcal{F}^{\mathrm{SSA}}_{\{\vec{R}_I\}}}{\partial R_J} = -\sum_m p_m \frac{\partial E^{\mathrm{BO}}(\{\vec{R}_I\},\vec{\sigma}_m)}{\partial R_J} \tag{2}$$

$$= \sum_m p_m \vec{F}^{\mathrm{HF}}_J(\{\vec{R}_I\},\vec{\sigma}_m). \tag{3}$$

Here, $\vec{F}^{\mathrm{HF}}_J(\{\vec{R}_I\},\vec{\sigma}_m)$ are the Hellmann-Feynman forces for an individual magnetic configuration $\vec{\sigma}_m$ and $p_m = \exp[-E^{\mathrm{BO}}(\{\vec{R}_I\},\vec{\sigma}_m)/k_{\mathrm{B}}T]/Z$ denotes the Boltzmann weights. The forces for each magnetic state can be regarded as fluctuations around the SSA forces

$$\vec{F}^{\mathrm{HF}}_J(\{\vec{R}_I\},\vec{\sigma}_m) = \vec{F}^{\mathrm{SSA}}_{J,\{\vec{R}_I\}} + \delta\vec{F}^{\mathrm{HF}}_J(\{\vec{R}_I\},\vec{\sigma}_m). \tag{4}$$

The impact of the fluctuation term $\delta\vec{F}^{\mathrm{HF}}_J(\{\vec{R}_I\},\vec{\sigma}_m)$ on the SSA forces $\vec{F}^{\mathrm{SSA}}_{J,\{\vec{R}_I\}}$ is directly related to the time scale of
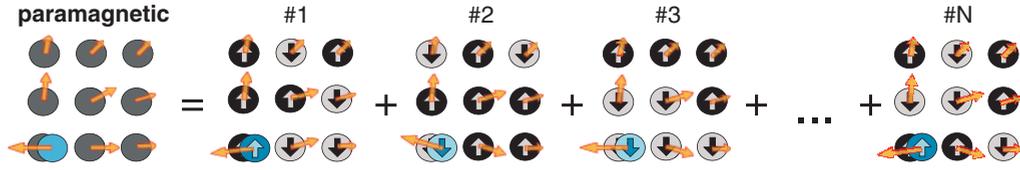
FIG. 1. (Color online) Sketch of the randomized magnetic SQS. The forces are indicated by orange arrows.

magnetic and atomic degrees of freedom. For the common case that magnetic moment oscillations are fast compared to atomic oscillations the magnetic induced fluctuations $\delta \vec{F}_J^{\mathrm{HF}}(\{\vec{R}_I\}, \vec{\sigma}_m)$ average out. The actual forces experienced by the atoms will thus be the effective averaged $\vec{F}_{J,\{\vec{R}_I\}}^{\mathrm{SSA}}$ rather than $\vec{F}_J^{\mathrm{HF}}(\{\vec{R}_I\}, \vec{\sigma}_m)$. The above formulation is general and allows one to compute the atomic forces by fully including finite temperature magnetism.

In order to test the reliability and applicability of the proposed approach, we apply it to the hitherto unsolved problem of computing phonons in the paramagnetic (PM) regime. As a material system we chose one of the best studied magnetic materials, pure iron. Although vibronic excitations in iron have been studied intensively both experimentally as well as theoretically for decades,[1,5,6,8,11,21,22] many basic questions still remain open. In particular, the impact of magnetism on lattice vibrations and phase stability is poorly understood up to now.[5,8,11,22,29] In the following we consider the paramagnetic β (bcc) and γ (fcc) phases of iron. For these high-temperature phases a long-time question is the source of stabilization, i.e., whether vibronic (phonons)[22] or magnetic excitations (magnons)[29] drive the phase transition and stabilize the high-temperature fcc phase.

In the high-temperature paramagnetic state the local magnetic moments are randomly distributed over the lattice as sketched in Fig. 1 and fluctuate in size and direction. Since at present DFT implementations are limited in computing accurate forces for constrained noncollinear magnetic structures, we simplify the modeling of the paramagnetic state by considering collinearly disordered magnetic moments. The SSA procedure is therefore performed employing a sufficiently large set of such randomly disordered collinear configurations $\{\vec{\sigma}_m\}$. These configurations are constructed using the concept of special quasirandom structures (SQSs) as obtained from the ATAT package.[30] We note, however, that the proposed scheme itself is very general and would, in principle, allow the incorporation of noncollinear structures, if technically realizable.

To compute the phonon spectra we employ the direct force constant method. Specifically, we diagonalize the force constant matrix $\phi_{\alpha\beta} := -\partial F_\alpha^{\mathrm{HF}}/\partial u_\beta$ created by the individual displacements u_β as sketched by the blue atoms in Fig. 1. The indices α and β go over all degrees of freedom of the atomic system. For a nonmagnetic (NM) calculation, the force constant matrix satisfies the underlying lattice symmetries S (point and translational symmetries), i.e.,

$$\phi_{\alpha\beta}^{\mathrm{NM}} = \sum_{\gamma\delta} S_{\alpha\gamma}^{\beta(\lambda)\delta} \phi_{\gamma\delta}^{\mathrm{NM}}, \tag{5}$$

where λ numerates all symmetry operators S providing symmetry equivalent atomic force constants.

It is crucial to note that switching on magnetism and considering an *individual magnetic* configuration the above symmetry will be destroyed. The resulting force constant matrix $\phi_{\alpha\beta}(\vec{\sigma}_m)$ therefore no longer has the symmetry of an fcc or bcc crystal. As a consequence, diagonalization of the corresponding dynamical matrix results in unstable (imaginary) phonon modes. Applying the SSA scheme restores the full atomic symmetry in the force constant matrix, i.e., $\phi_{\alpha\beta}^{\mathrm{SSA}}$ has the same symmetry as $\phi_{\alpha\beta}^{\mathrm{nm}}$ and thus obeys Eq. (5). This observation can be used to derive the following equivalence between symmetrization and spin averaging:

$$\phi_{\alpha\beta}^{\mathrm{sym}} = \sum_\lambda \sum_{\gamma\delta} S_{\alpha\gamma}^{\beta(\lambda)\delta} \phi_{\gamma\delta}(\vec{\sigma}_{m_0}) \tag{6}$$

$$= \sum_\lambda \phi_{\alpha\beta}(\vec{\sigma}_{\lambda(m_0)}) = \phi_{\alpha\beta}^{\mathrm{SSA}}, \tag{7}$$

where $\vec{\sigma}_{\lambda(m_0)}$ denotes the magnetic configuration after applying the symmetry operation. The above equivalence allows one to perform the full SSA using a single magnetic configuration $\vec{\sigma}_{m_0}$ provided that (i) the number of symmetry operations $\lambda(m_0)$ is sufficiently large and (ii) $\vec{\sigma}_{m_0}$ is constructed such that it resembles a large number of *locally* inequivalent magnetic configurations. Note that due to the fact that all displacements are computed in the same supercell, the total energies entering the Boltzmann factor in Eq. (1) are identical (degenerate), i.e., all magnetic configurations have the same weight. If the number of symmetry operations λ is not sufficient to obtain converged SSA force constants, the above formalism can be straightforwardly extended by replacing the single initial magnetic configuration $\vec{\sigma}_{m_0}$ by a set of $\vec{\sigma}_{m_i}$ where the index i marks symmetry inequivalent magnetic configurations.

Before applying our approach, we first show results obtained from two common treatments for phonon spectra of paramagnetic bcc and fcc iron. These are based on ferromagnetic (FM) and NM calculations. All DFT calculations in the following are performed using the VASP[32] package employing the projector augmented-wave method[33] within the generalized gradient approximation (Perdew-Burke-Ernzerhof parametrization[34]).[35]

The first approximation (FM) assumes that even at high temperatures, where the magnetic order is destroyed, it is still possible to use the magnetic ground state, e.g., the ferromagnetically saturated state for bcc iron.[9,11,13,20] The theoretical calculations are carried out at the experimental volume at the considered temperatures.[36] This allows one to test the performance and applicability of our approach. The ultimate goal is of course a fully theoretical determination of the equilibrium lattice constant at the considered temperature. The proposed SSA scheme itself is a mandatory step in this
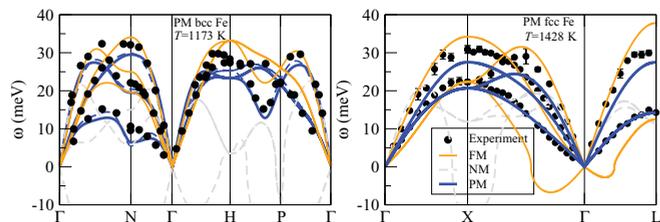
FIG. 2. (Color online) Phonon spectra for paramagnetic bcc and fcc iron in comparison with experimental data (Refs. 22,31). In addition the results obtained from a ferromagnetic (FM) and a nonmagnetic (NM) calculation are shown.

FIG. 3. (Color online) Left panels: Convergence of the mean value of the force on the displaced atom $F_{A_i}^{A_i}$ and its nearest neighbor $F_{A_{nn}}^{A_i}$. Right panels: Density of states of force constants due to individual displacements.

direction, since vibronic contributions are the basic driving force of volume expansion. In fcc iron interesting magnetovolume effects[8,37,38] are observed. These are particularly prominent at $T = 0$ K and result, e.g., in a highly sensitive dependence of magnetic interactions on volume[38] or in a strong dependence of elastic properties on the magnetic state.[37] In the high-temperature paramagnetic limit, which is in the focus of the present paper, such effects are likely to be averaged out. This is in agreement with recent DMFT calculations by Leonov *et al.*,[28] where paramagnetic phonons at a lower lattice constant are computed and found to be in good agreement with our results. In Fig. 2 the results at high temperature ($T_{\text{exp}} = 1173$ and 1428 K) obtained for a FM calculation for bcc and fcc iron (orange lines) are shown in comparison with experimental data. Both temperatures are above the critical magnetic temperature of bcc and fcc iron, respectively. In the case of bcc iron, the longitudinal branches are in reasonable agreement with experiment. However, the experimentally observed pronounced softening at high temperatures, in particular of the transversal modes (T) between H and P as well as between Γ and N are not reproduced. The softening of the latter modes is directly related to a strong decrease in the elastic constants C' and C_{11}. These elastic constants are directly involved in the structural transformation path (Bain path) from bcc to fcc, and, e.g., critical to understand mechanical failure of ferritic steels at high T.

The difference between experiment and this level of theory is even more pronounced for fcc iron.[39] Here the calculations provide imaginary phonon frequencies for the modes between Γ and X, and Γ and L consistent with structural instability of FM fcc iron with respect to tetragonal deformation.[38,40]

The second approximation to approximate the paramagnetic states is to perform NM (i.e., non-spin-polarized) calculations. This approximation is based on the Stoner theory of magnetism.[41] According to this model, magnetic moments remain ferromagnetically ordered for the whole temperature range $0 < T < T_C$. With increasing temperature the magnitude of the local moments decreases and finally vanishes for $T \geqslant T_C$. To elucidate how such an approach performs in the case of iron we show the results of NM calculations in Fig. 2 (gray lines). The results are very similar to recent calculations employing ultrasoft pseudopotentials.[6,21] For both bcc and fcc iron, unstable (imaginary) phonon modes appear. For bcc iron, the softening appears around the Γ point consistent with a negative shear elastic constant (C').[40]
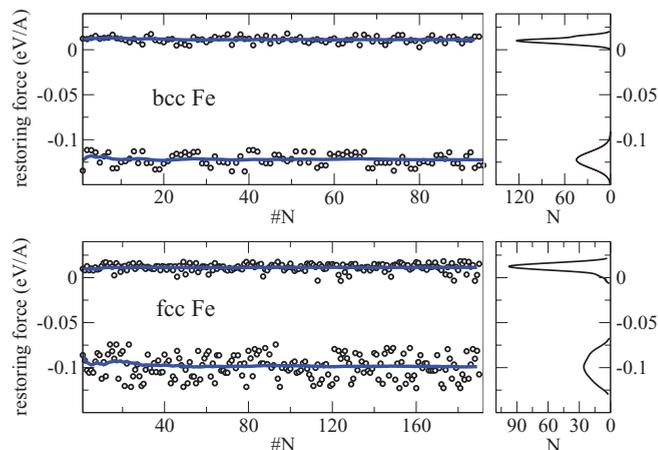
Summarizing, neither of the two existing approaches, i.e., approximating the PM state by FM or NM calculations, provides an accurate description of the vibrational frequencies.

As a first step to test our proposed approach we set up a 16 atomic spin SQS for bcc iron (sketched in Fig. 1) with the atoms in the ideal bcc positions. For this fixed spin configuration we obtain nonvanishing atomic forces, i.e., the magnetically disordered structure is unstable at $T = 0$ K and atomic relaxation would destroy the bcc symmetry. In a second step we compute the atomic forces for all inequivalent displacements. After employing the SSA procedure [Eq. (7)], we obtain the force on the displaced atoms as well as the force on its nearest neighbor (Fig. 3, upper panel). The individual forces $\vec{F}_{J,\Delta}^{\text{HF}}(\vec{\sigma}_{\lambda(m_0)})$ [Eq. (4)] fluctuate around the mean SSA value $\vec{F}_{J,\Delta}^{\text{SSA}}$ as can be also seen in the force density of states (right panel in Fig. 3). Δ denotes the change of the atomic positions from the ideal to the displaced configuration used in the force calculation. We can thus conclude that a single SQS provides a sufficient set of magnetic configurations if the lattice symmetries are employed.

From the effective force constants the phonon dispersions for bcc iron are computed and shown in Fig. 2 (left panel, blue line). First, it can be seen that no imaginary phonon frequencies occur in contrast to the nonmagnetic calculations. The overall dispersions are shifted to lower energies as compared to the ferromagnetic solution and significantly improve the agreement with experiment. In particular, the strong softening of the transversal ΓN modes as well as the softening around the dip in the HP branches are now well reproduced and clearly demonstrate the large impact magnetic disorder has on the vibrational properties of bcc iron.

To estimate the impact of supercell size convergence we performed the same procedure starting from a 54 atomic bcc SQS. The obtained phonon spectra are also shown in Fig. 2 (dashed blue line). The corresponding spectrum is slightly shifted to lower frequencies. The overall correction is about one order of magnitude smaller than the impact of the magnetic state and thus for the present analysis, negligible.

We now discuss the fcc phase of Fe. As discussed in the beginning, neither FM nor NM calculations are sufficient to correctly reproduce the experimental data. The calculations are performed using a 32 atomic SQS. All 32×6 inequivalent displacements giving in total $N = 192$ individual snapshots $\vec{\sigma}_{\lambda(m_0)}$ for the statistical average equation (4) are included. The performance of the spin-averaging procedure on the forces is shown in Fig. 3, lower panel. Similar as for bcc iron, we obtain a rapid convergence of the averaged forces by including more and more individual snapshots. From the averaged force matrix we deduce the phonon spectrum for fcc iron. Overall the obtained dispersion is in excellent agreement with experimental data. Compared to the FM solution, dominantly the longitudinal branches are shifted to lower values, whereas the transversal branches are shifted to higher frequencies, removing the instability around the Γ point. We can thus conclude that PM suffices to make fcc iron metastable.

In conclusion, we propose an approach that allows one to compute atomic forces for magnetic systems at finite T and that can be easily connected to existing DFT codes. To test the reliability and performance of the proposed approach, phonon spectra of PM β (bcc) and γ (fcc) iron are computed. Our results clearly demonstrate that magnetic disorder alone, i.e., without having to invoke high-temperature anharmonic contributions, guarantees dynamic stability of the iron fcc phase. In the absence of a realistic paramagnetic description, i.e., considering fcc Fe in a ferro- or nonmagnetic state, unphysical imaginary phonon modes arise. This clearly demonstrates the strong interplay of atomic and magnetic degrees of freedom involved in the stability mechanisms in iron and the importance to perform phonon calculations based on the actual (realistic) magnetic phases. The approach can be easily extended to structures with reduced symmetries (e.g., point or extended defects) or to perform MD calculations including finite temperature magnetism. MD calculations will largely profit from a straightforward parallelization over disordered magnetic configurations.

*koermann@mpie.de

[1] H. K. Mao, J. Xu, V. V. Struzhkin, J. Shu, R. J. Hemley, W. Sturhahn, M. Y. Hu, E. E. Alp, L. Vočadlo, D. Alfé, G. D. Price, M. J. Gillan, M. Schwoerer-Böhning, D. Häusermann, P. Eng, G. Shen, H. Giefers, R. Lübbers, and G. Wortmann, Science **292**, 914 (2001).

[2] M. A. Uijttewaal, T. Hickel, J. Neugebauer, M. E. Gruner, and P. Entel, Phys. Rev. Lett. **102**, 035702 (2009).

[3] L. Vitos, P. A. Korzhavyi, and B. Johansson, Nat. Mater. **2**, 25 (2003)

[4] C. M. Fang, M. H. F. Sluiter, M. A. van Huis, C. K. Ande, and H. W. Zandbergen, Phys. Rev. Lett. **105**, 055503 (2010).

[5] J. Łażewski, P. Piekarz, A. M. Oleś, and K. Parlinski, Phys. Rev. B **74**, 174304 (2006).

[6] W. Zhang, J. Magn. Magn. Mater. **323**, 2206 (2011).

[7] M. Y. Lavrentiev, D. Nguyen-Manh, and S. L. Dudarev, Phys. Rev. B **81**, 184202 (2010).

[8] R. F. Sabiryanov and S. S. Jaswal, Phys. Rev. Lett. **83**, 2062 (1999).

[9] F. Körmann, A. Dick, T. Hickel, and J. Neugebauer, Phys. Rev. B **81**, 134425 (2010).

[10] A. Dick, F. Körmann, T. Hickel, and J. Neugebauer, Phys. Rev. B **84**, 125101 (2011).

[11] F. Körmann, A. Dick, B. Grabowski, B. Hallstedt, T. Hickel, and J. Neugebauer, Phys. Rev. B **78**, 033102 (2008).

[12] F. Körmann, A. Dick, T. Hickel, and J. Neugebauer, Phys. Rev. B **79**, 184406 (2009).

[13] F. Körmann, A. Dick, T. Hickel, and J. Neugebauer, Phys. Rev. B **83**, 165114 (2011).

[14] B. Grabowski, T. Hickel, and J. Neugebauer, Phys. Status Solidi B **248**, 1295 (2011).

[15] D. Alfé, M. J. Gillan, and G. D. Price, Nature (London) **401**, 462 (1999).

[16] A. B. Belonoshko, P. I. Dorogokupets, B. Johansson, S. K. Saxena, and L. Koči, Phys. Rev. B **78**, 104107 (2008).

[17] L. Vočadlo and D. Alfè, Phys. Rev. B **65**, 214105 (2002).

[18] A. van de Walle and G. Ceder, Rev. Mod. Phys. **74**, 11 (2002).

[19] B. Grabowski, L. Ismer, T. Hickel, and J. Neugebauer, Phys. Rev. B **79**, 134106 (2009).

[20] X. Sha and R. E. Cohen, Phys. Rev. B **73**, 104303 (2006).

[21] H. C. Hsueh, J. Crain, G. Y. Guo, H. Y. Chen, C. C. Lee, K. P. Chang, and H. L. Shih, Phys. Rev. B **66**, 052420 (2002).

[22] J. Neuhaus, W. Petry, and A. Krimmel, Physica B **234–236**, 897 (1997).

[23] H. Hasegawa, M. W. Finnis, and D. G. Pettifor, J. Phys. F: Met. Phys. **17**, 2049 (1987).

[24] A. V. Ruban and I. A. Abrikosov, Rep. Prog. Phys. **71**, 046501 (2008).

[25] B. L. Gyorffy, A. J. Pindor, J. Staunton, G. M. Stocks, and H. Winter, J. Phys. F **15**, 1337 (1985).

[26] S.-L. Shang, Y. Wang, and Z.-K. Liu, Phys. Rev. B **82**, 014425 (2010).

[27] M. Pajda, J. Kudrnovsky, I. Turek, V. Drchal, and P. Bruno, Phys. Rev. B **64**, 174402 (2001).

[28] I. Leonov, A. I. Poteryaev, V. I. Anisimov, and D. Vollhardt, Phys. Rev. B **85**, 020401 (2012).

[29] H. Hasegawa and D. G. Pettifor, Phys. Rev. Lett. **50**, 130 (1983).

[30] A. van de Walle and G. Ceder, J. Phase Equilib. **23**, 348 (2002).

[31] J. Zarestky and C. Stassis, Phys. Rev. B **35**, 4500 (1987).

[32] G. Kresse and J. Furthmüller, Phys. Rev. B **54**, 11169 (1996).

[33] P. E. Blöchl, Phys. Rev. B **50**, 17953 (1994)

[34] J. P. Perdew, K. Burke, and M. Ernzerhof, Phys. Rev. Lett. **77**, 3865 (1996).

[35] Calculations include up to 54 atoms for bcc and 32 atoms for fcc iron. Up to 12000 **k** points per atom and a plane-wave cutoff energy of $E_{cut} = 340$ eV has been chosen to ensure converged phonon spectra (< 1 meV).

[36] M. Acet, H. Zähres, E. F. Wassermann, and W. Pepperhoff, Phys. Rev. B **49**, 6012 (1994).

[37] H. C. Herper, E. Hoffmann, and P. Entel, Phys. Rev. B **60**, 3839 (1999).

[38] S. V. Okatov, A. R. Kuznetsov, Y. N. Gornostyrev, V. N. Urtsev, and M. I. Katsnelson, Phys. Rev. B **79**, 094111 (2009).

[39] Note that the theoretically lowest collinear magnetic state for fcc iron is given by an antiferromagnetic configuration.

[40] M. Friák, M. Šob, and V. Vitek, Phys. Rev. B **63**, 052405 (2001).

[41] T. Moriya, J. Magn. Magn. Mater. **100**, 261 (1991).